Optimal Planning of Voltage Sag in A Power System with Specially Connected Transformers Considering ITI Curve

Ying-Pin Chang

Department of Electrical Engineering, Nan Kai University of Technology

通訊作者：張英彬
聯絡地址：南投縣草屯鎮中正路 568 號
電子郵件：cyp@nkut.edu.tw
投稿日期：2012 年 1 月
接受日期：2012 年 4 月

Abstract

This paper examined the voltage sag planning of a power system with V-V, Scott, and Le Blanc connected transformers by using the ant direction hybrid differential evolution (ADHDE) method. The analysis considered the ITI (CBEMA) curve and coordination of over-current relays. Firstly, the equivalent node admittance matrix model for calculation of voltage sag was investigated to obtain the sag severity of the system after single or two-phase faults. The analytical equations were useful in the mathematical method and optimal planning for balance and unbalance faults of specially connected transformers. Then, the effect of over-current relay setting on the duration of voltage sag was discussed. The ADHDE was used to obtain the suitable transformer impedances. The relay time multiplier parameter was also a variable. The test on the power systems with V-V, Scott, and Le Blanc connected transformers scheme was chosen to show the effectiveness of this method. The results showed that the voltage sag severity could be improved by the tuning of transformer impedances and relay settings. Finally, this paper showed the optimal transformer reactance values X_{TRS}=7%, system reactance values X_{TRL}=16%, and over-current relay settings k=0.01 was determined by using the ADHDE approach and fault voltage, fault current, fault clearing time, and objective function were 0.6456 p.u., 14.41 p.u, 0.10554 s, and 0.0543 p.u., respectively for the 69kV bus at the V_A (V-V) phase. Although the V_A(Le Blanc) phase objective function was as high as 0.0833(p.u.), fault voltage, fault current, fault clearing time were satisfied. Because the emigrant, accelerated and mutation operators were embedded in ADHDE, a global optimum and faster convergence were achieved.

Keywords： voltage sag, power quality, ITI (CBEMA) curve, ant direction hybrid differential evolution method, specially connected transformers

1. Introduction

The voltage sag is one of indexes of power quality degradation and a useful measure of the fault events. Some momentary faults would cause voltage sag during the transient period until protective relay are activated, and the circuit breakers clean the faults. The voltage sag study the voltage values in the system reduce to between 10% and 90% of the normal values in a period of a few cycles by Bollen (1999) and IEEE Std. 446-1995 [1-2]. The voltage sag magnitude and duration are the essential characteristics. It comprises two parts: the drop in the voltage (ΔV) such as IEEE Std. (2006), IEEE Std. 1159-1995, Das (1990), Bollen (1995) and the duration (Δt) such as Bollen (1997), Yalcinkaya, Bollen, and Crossley (1998). While ΔV is determined by the system impedances and fault types, and Δt is determined by the protective relays and the action of the circuit breakers. This phenomenon can be expressed as the rectangular area in Fig. 1. It can define the voltage sag severity as $\Delta V \Delta t$. Relevant limits on voltage sag are defined for consumer electronic products, large electrical equipments, and semiconductor manufacturing machines. The Information Technology Industry Council, Computer Business Equipment Manufacturers Association (ITI, CBEMA) has suggested the curve, as plotted in Fig. 2 by Gomez and Morcos (2002) and Conrad, Bollen (1997) and Kyei, Ayanar, Heydt, and Thallam (2002) and Heydt, Ayyanar, and Thallam (1994) and Gomez and Morcos (2002). Additionally, the Semiconductor Equipment and Materials International (SEMI) also have developed the SEMI curve to define the ability of semiconductor devices and equipment during voltage sag.

Some special electrical systems usually require strong single-phase power sources. To reduce the voltage unbalance disturbances to the three-phase sources, some specially connected transformers are used, such as V-V, Scott, and Le Blanc connection schemes. Some schemes have been employed in the railway electrification systems. The power quality issues in railway electrification systems include the studies on the influence of traction loads on three-phase utility systems. For example, simplified models of specially connected transformers have been studied in three-phase power flow studies such as Chen (1994), and Chen and Kuo (1995) presents a network model was proposed for investigating unbalance effects. Huang, Kuo, Chan, Lu, and Huang (2001) used a short circuit current study for power supply system.

However, related issues having not been addressed voltage sag of power quality, include the specially connected transformers equivalent simplified model for three-phase power flow, and the EMTP based network model with unbalance effects, and the EMTP study short circuit current for power flow. In this paper, the short circuit voltages and currents of specially connected transformers calculated by node admittance matrix mathematical models. Then the voltage sag planning is investigated by using the method of ADHDE (refer to the appendix), which is a direct and parallel search method that involves accelerating and migrant operations to prevent falling into local optimal solutions by Lee, Albu, and Heydt (2004) and Heydt and Jewell (1998) and Chang and Wu (2005) and Chiou and Wang (1998) and Lin, Hwang, and Wang (1999, 2000). Chang and Low, (2008) presents an ADHDE presents a heuristic which combines the orthogonal array experiment technique and an ant direction hybrid differential evolution algorithm (ADHDEOA) for planning of a large-scale passive harmonic filters problem. The addressed problem has a multi-bus and under abundant harmonic current sources in the system. In this study, an orthogonal array is first conducted to obtain the initial solution. Next, an ant direction hybrid differential evolution (ADHDE) is applied to search for a near optimum solution. In this study, the ADHDE method utilizes the concept of ant colony search to search the proper mutation operator to accelerate searching out the global solution for system equipment parameters over a wide range, such as the transformer impedances and protective relay time multiple settings are variables. Calculation values are compared with the of ITI (CBEMA) curve. From the simulation results, this paper is organized as follows voltage sag. That introduces the voltage sag architecture models of the specially connected transformers. Next, the article illustrates the investigating procedure and results. Finally, the voltage sag severity of a power system with specially connected transformer can be greatly improved by the purposed method.

2. Methods

2.1 Equivalent Admittance Network Modeling of Transformers

The analytical models of the three-phase to two-phase

specially connected transformers are required in the optimal design procedure. There are three connection schemes, which are V-V, Scott and Le Blanc. The models are developed in winding connections and phase coordinates, considering the copper loss and phase-angle displacement between primary and secondary voltages. Let $k_1 = \frac{N_1}{N_2}$ and $k_2 = \frac{N_2}{N_1}$ denote the turn ratios of each phase. The y_t represents the equivalent admittance of series impedance of each single-phase transformer obtained in the short circuit test.

2.1.1 V-V connection

The V-V connection scheme, as shown in Fig. 3, is composed of two single-phase transformers. It uses three-phase power on the primary side, and supplies two single-phase loads on the secondary side, which are the main transform (M) and the teaser transformer (T). Then the phasor voltages and currents are given by

$$\begin{bmatrix} V_T \\ V_M \end{bmatrix} = k_2 \begin{bmatrix} 1 & -1 & 0 \\ 0 & 1 & -1 \end{bmatrix} \begin{bmatrix} V_A \\ V_B \\ V_C \end{bmatrix} \tag{1}$$

$$\begin{bmatrix} I_A \\ I_B \\ I_C \end{bmatrix} = k_2 \begin{bmatrix} 1 & 0 \\ -1 & 1 \\ 0 & -1 \end{bmatrix} \begin{bmatrix} I_T \\ I_M \end{bmatrix} \tag{2}$$

The equivalent circuit can be made available by the interconnection method, as shown Fig. 4. The node-voltage equation of the three-phase to two-phase transformer in matrix form is

$$\begin{bmatrix} I_A \\ I_B \\ I_C \\ I_{T1} \\ I_{T2} \\ I_{M1} \\ I_{M2} \end{bmatrix} = Y \begin{bmatrix} V_A \\ V_B \\ V_C \\ V_{T1} \\ V_{T2} \\ V_{M1} \\ V_{M2} \end{bmatrix} \tag{3}$$

where $I_{T2} = -I_{T1} = I_T$ and $I_{M2} = -I_{M1} = I_M$

The node admittance matrix (bus admittance matrix) can be expressed as

$$Y = \begin{array}{c} \\ A \\ B \\ C \\ T1 \\ T2 \\ M1 \\ M2 \end{array} \begin{array}{c} \begin{array}{ccccccc} A & B & C & T1 & T2 & M1 & M2 \end{array} \\ \begin{bmatrix} y_t & -y_t & 0 & -y_t & y_t & 0 & 0 \\ 0 & 2y_t & -y_t & y_t & -y_t & -y_t & y_t \\ 0 & -y_t & y_t & 0 & 0 & y_t & -y_t \\ -y_t & y_t & 0 & y_t & -y_t & 0 & 0 \\ y_t & -y_t & 0 & -y_t & y_t & 0 & 0 \\ 0 & -y_t & y_t & 0 & 0 & y_t & -y_t \\ 0 & y_t & -y_t & 0 & 0 & -y_t & y_t \end{bmatrix} \end{array} \tag{4}$$

The limitation with V -V connection are given below :

1. The average p.f. at which V- V bank is operating is less than that with the load. This power factor (or p. f.) is 86.6 % of the balanced load p.f.
2. The tow transformers in V -V bank operate at different power factor except for balanced unity p.f .load.
3. The terminals voltages available on the secondary side become unbalanced. This may happen eventhough load is perfectly balanced. Thus in summary we can say that if tow transformers are connected in V - V fashion and are loaded to rated capacity and one transformer is added to increase the total capacity by $\sqrt{3}$ or 173.2 %. Thus the increase in capacity is 73.2 % when converting from a V-V system to a Δ-Δ system.

2.1.2 Scott connection

Fig. 5 shows the Scott connection scheme, comprising of two different turn ratio transformers. The main transform (phase M) has a center-tapped winding on the primary side, and a single winding on the secondary side. The teaser transformer (phase T) is a single-phase transformer. The phase difference between M and T is 90°. The phasor voltages and currents can be expressed as follow

$$\begin{bmatrix} V_T \\ V_M \end{bmatrix} = k_2 \begin{bmatrix} 2/\sqrt{3} & -1/\sqrt{3} & -1/\sqrt{3} \\ 0 & 1 & -1 \end{bmatrix} \begin{bmatrix} V_A \\ V_B \\ V_C \end{bmatrix} \tag{5}$$

$$\begin{bmatrix} I_A \\ I_B \\ I_C \end{bmatrix} = k_2 \begin{bmatrix} 2/\sqrt{3} & 0 \\ -1/\sqrt{3} & 1 \\ -1/\sqrt{3} & -1 \end{bmatrix} \begin{bmatrix} I_T \\ I_M \end{bmatrix} \tag{6}$$

The equivalent circuit model can also be obtained by the interconnection method, as shown Fig. 6. The node admittance matrix of this scheme can be expressed as

$$Y=\begin{array}{c} \begin{matrix} A & B & C & T1 & T2 & M1 & M2 \end{matrix} \\ \begin{bmatrix} \frac{8}{9}y_t & \frac{-4}{9}y_t & \frac{-4}{9}y_t & \frac{-4\sqrt{3}}{9}y_t & \frac{4\sqrt{3}}{9}y_t & 0 & 0 \\ \frac{-4}{9}y_t & \frac{20}{9}y_t & \frac{-16}{9}y_t & \frac{2\sqrt{3}}{9}y_t & \frac{-2\sqrt{3}}{9}y_t & -2y_t & 2y_t \\ \frac{-4}{9}y_t & \frac{-16}{9}y_t & \frac{20}{9}y_t & \frac{2\sqrt{3}}{9}y_t & \frac{-2\sqrt{3}}{9}y_t & 2y_t & -2y_t \\ \frac{-4\sqrt{3}}{9}y_t & \frac{2\sqrt{3}}{9}y_t & \frac{2\sqrt{3}}{9}y_t & \frac{2}{3}y_t & \frac{-2}{3}y_t & 0 & 0 \\ \frac{4\sqrt{3}}{9}y_t & \frac{-2\sqrt{3}}{9}y_t & \frac{-2\sqrt{3}}{9}y_t & \frac{-2}{3}y_t & \frac{2}{3}y_t & 0 & 0 \\ 0 & -2y_t & 2y_t & 0 & 0 & 2y_t & -2y_t \\ 0 & 2y_t & -2_t & 0 & 0 & -2y_t & 2y_t \end{bmatrix} \begin{matrix} A \\ B \\ C \\ T1 \\ T2 \\ M1 \\ M2 \end{matrix} \end{array} \tag{7}$$

Assuming the desired voltage is the same on the two and three phase sides, the Scott transformer connection consists of a center-tapped ratio at main transformer, and an 86.6% ($0.5\sqrt{3}$) ratio teaser transformer. The center-tapped side of Tr. is connected between two of the phases on the three-phase side. Its center tap then connects to one end of the lower turn count side of Tr. the other end connects to the remaining phase. The other side of the transformers then connect directly to the two pairs of a two-phase four-wire system.

2.1.3 Le Blanc connection

The connection diagram of the Le Blanc scheme is given in Fig. 7. The primary windings are the same as those of a general three-phase transformer in the delta connection. The secondary side consists of five windings, which are separated into two phases. The phasor voltages and currents are given by

$$\begin{bmatrix} V_T \\ V_M \end{bmatrix} = k_2 \begin{bmatrix} -2/\sqrt{3} & 1/\sqrt{3} & 1/\sqrt{3} \\ 0 & 1 & -1 \end{bmatrix} \begin{bmatrix} V_A \\ V_B \\ V_C \end{bmatrix} \tag{8}$$

$$\begin{bmatrix} I_A \\ I_B \\ I_C \end{bmatrix} = k_2 \begin{bmatrix} -2/\sqrt{3} & 0 \\ 1/\sqrt{3} & 1 \\ 1/\sqrt{3} & -1 \end{bmatrix} \begin{bmatrix} I_T \\ I_M \end{bmatrix} \tag{9}$$

The equivalent circuit can also be made by the interconnection method, as shown Fig. 8. The node admittance matrix of this scheme be expressed as

$$Y=\begin{array}{c} \begin{matrix} A & B & C & T1 & T2 & M1 & M2 \end{matrix} \\ y_t \begin{bmatrix} 3-\sqrt{3} & \frac{-(3-\sqrt{3})}{2} & \frac{-(3-\sqrt{3})}{2} & \frac{3(\sqrt{3}-1)}{2} & \frac{-3(\sqrt{3}-1)}{2} & 0 & 0 \\ \frac{-(3-\sqrt{3})}{2} & 3-\sqrt{3} & \frac{-3(3-\sqrt{3})}{2} & \frac{-3(\sqrt{3}-1)}{4} & \frac{3(\sqrt{3}-1)}{4} & \frac{3(3-\sqrt{3})}{4} & \frac{-3(3-\sqrt{3})}{4} \\ \frac{-(3-\sqrt{3})}{2} & \frac{-3(3-\sqrt{3})}{2} & 3-\sqrt{3} & \frac{-3(\sqrt{3}-1)}{4} & \frac{3(\sqrt{3}-1)}{4} & \frac{-3(3-\sqrt{3})}{4} & \frac{3(3-\sqrt{3})}{4} \\ \frac{3(\sqrt{3}-1)}{2} & \frac{-3(\sqrt{3}-1)}{4} & \frac{-3(\sqrt{3}-1)}{4} & \frac{3(3-\sqrt{3})}{4} & \frac{-3(3-\sqrt{3})}{4} & 0 & 0 \\ \frac{-3(\sqrt{3}-1)}{2} & \frac{3(\sqrt{3}-1)}{4} & \frac{3(\sqrt{3}-1)}{4} & \frac{-3(3-\sqrt{3})}{4} & \frac{3(3-\sqrt{3})}{4} & 0 & 0 \\ 0 & \frac{3(3-\sqrt{3})}{4} & \frac{-3(3-\sqrt{3})}{4} & 0 & 0 & \frac{3(3-\sqrt{3})}{4} & \frac{-3(3-\sqrt{3})}{4} \\ 0 & \frac{-3(3-\sqrt{3})}{4} & \frac{3(3-\sqrt{3})}{4} & 0 & 0 & \frac{-3(3-\sqrt{3})}{4} & \frac{3(3-\sqrt{3})}{4} \end{bmatrix} \begin{matrix} A \\ B \\ C \\ T1 \\ T2 \\ M1 \\ M2 \end{matrix} \end{array} \tag{10}$$

The primary side of the Le Blanc transformer is a connection winding, its secondary side uses an unbalanced winding structure (phases and have two secondary side windings; however, phase has only one winding). The secondary side output voltage and current has a 90 phase angle difference.

2.2 Short Circuit Fault Calculation

The per-unit values are used in the calculation. Fig. 9 shows a power system with a three-phase to two-phase transformer. The source is a balanced three-phase Y connection 161 kV power system. There are three voltage levels such as 161 kV, 69 kV, and 27.5 kV, respectively.

The equivalent model for short circuit calculation of a power system with specially connected transformers is given in Fig. 10. Let the source voltages be

$$\begin{aligned} V_{SA} &= \frac{V}{\sqrt{3}}\angle 0° \\ V_{SB} &= \frac{V}{\sqrt{3}}\angle -120° \\ V_{SC} &= \frac{V}{\sqrt{3}}\angle 120° \end{aligned} \tag{11}$$

Then, the equivalent injected currents are expressed as

$$\begin{aligned} I_{SA} &= V_{SA} y_{src} \\ I_{SB} &= V_{SB} y_{src} \\ I_{SC} &= V_{SC} y_{src} \end{aligned} \tag{12}$$

where $y_{src} = Z_{src}^{-1} = (Z_S + Z_{TRS} + Z_{L1})^{-1}$ and Z_{TRS} is the series impedance of the 161/69 kV transformer. Then, the node-voltage equation of the study system is given by

$$\begin{bmatrix} I_A \\ I_B \\ I_C \\ I_{T1} \\ I_{T2} \\ I_{M1} \\ I_{M2} \end{bmatrix} = Y_e \begin{bmatrix} V_A \\ V_B \\ V_C \\ V_{T1} \\ V_{T2} \\ V_{M1} \\ V_{M2} \end{bmatrix} \tag{13}$$

The node admittance matrix of the study system can be obtained by

$$Y_e(i,j) = \begin{cases} Y(i,j) + y_T & i = j = 4,5 \\ Y(i,j) - y_T & i = 4, j = 5, or, i = 5, j = 4 \\ Y(i,j) + y_M & i = j = 6,7 \\ Y(i,j) - y_M & i = 6, j = 7, or, i = 7, j = 6 \\ Y(i,j) & others \end{cases} \tag{14}$$

where $y_T = Z_T^{-1} = (Z_{L2T} + Z_{TL})^{-1}$

$y_M = Z_M^{-1} = (Z_{L2M} + Z_{ML})^{-1}$

It can also be found that

$$\begin{aligned} V_A &= V_{SA} - \frac{I_A}{y_{src}} \\ V_B &= V_{SB} - \frac{I_B}{y_{src}} \\ V_C &= V_{SC} - \frac{I_C}{y_{src}} \\ V_{T2} &= V_{T1} - \frac{I_T}{y_T} \\ V_{M2} &= V_{M1} - \frac{I_M}{y_M} \\ I_{T2} &= -I_{T1} = I_T \\ I_{M2} &= -I_{M1} = I_M \\ V_T &= \frac{I_T}{y_T} \\ V_M &= \frac{I_M}{y_M} \end{aligned} \tag{15}$$

Substitute Eq. (15) into Eq.(13) can be obtained by

$$\begin{aligned} f_1(I_A, I_B, I_C, I_T, I_M, V_T, V_M) &= c_1 \\ f_2(I_A, I_B, I_C, I_T, I_M, V_T, V_M) &= c_2 \\ f_3(I_A, I_B, I_C, I_T, I_M, V_T, V_M) &= c_3 \\ f_4(I_A, I_B, I_C, I_T, I_M, V_T, V_M) &= c_4 \\ f_5(I_A, I_B, I_C, I_T, I_M, V_T, V_M) &= c_5 \\ f_6(I_A, I_B, I_C, I_T, I_M, V_T, V_M) &= c_6 \\ f_7(I_A, I_B, I_C, I_T, I_M, V_T, V_M) &= c_7 \end{aligned} \tag{16}$$

Using Taylor's series was

$$\Delta C^{(k)} = J^{(k)} \Delta X^{(k)} \tag{17}$$

$$X^{(k+1)} = X^{(k)} + \Delta X^{(k)} \tag{18}$$

where

$$\Delta X^{(k)} = \begin{bmatrix} \Delta I_A^{(k)} \\ \Delta I_B^{(k)} \\ \Delta I_C^{(k)} \\ \Delta I_T^{(k)} \\ \Delta I_M^{(k)} \\ \Delta V_T^{(k)} \\ \Delta V_M^{(k)} \end{bmatrix} \quad \text{and} \quad \Delta C^{(k)} = \begin{bmatrix} c_1 - (f_1)^{(k)} \\ c_2 - (f_2)^{(k)} \\ c_3 - (f_3)^{(k)} \\ c_4 - (f_4)^{(k)} \\ c_5 - (f_5)^{(k)} \\ c_6 - (f_6)^{(k)} \\ c_7 - (f_7)^{(k)} \end{bmatrix} \tag{19}$$

$$J^{(k)}=\begin{bmatrix}
(\frac{\partial f_1}{\partial I_A})^{(k)} & (\frac{\partial f_1}{\partial I_B})^{(k)} & (\frac{\partial f_1}{\partial I_C})^{(k)} & (\frac{\partial f_1}{\partial I_T})^{(k)} & (\frac{\partial f_1}{\partial I_M})^{(k)} & (\frac{\partial f_1}{\partial V_T})^{(k)} & (\frac{\partial f_1}{\partial V_M})^{(k)} \\
(\frac{\partial f_2}{\partial I_A})^{(k)} & (\frac{\partial f_2}{\partial I_B})^{(k)} & (\frac{\partial f_2}{\partial I_C})^{(k)} & (\frac{\partial f_2}{\partial I_T})^{(k)} & (\frac{\partial f_2}{\partial I_M})^{(k)} & (\frac{\partial f_2}{\partial V_T})^{(k)} & (\frac{\partial f_2}{\partial V_M})^{(k)} \\
(\frac{\partial f_3}{\partial I_A})^{(k)} & (\frac{\partial f_3}{\partial I_B})^{(k)} & (\frac{\partial f_3}{\partial I_C})^{(k)} & (\frac{\partial f_3}{\partial I_T})^{(k)} & (\frac{\partial f_3}{\partial I_M})^{(k)} & (\frac{\partial f_3}{\partial V_T})^{(k)} & (\frac{\partial f_3}{\partial V_M})^{(k)} \\
(\frac{\partial f_4}{\partial I_A})^{(k)} & (\frac{\partial f_4}{\partial I_B})^{(k)} & (\frac{\partial f_4}{\partial I_C})^{(k)} & (\frac{\partial f_4}{\partial I_T})^{(k)} & (\frac{\partial f_4}{\partial I_M})^{(k)} & (\frac{\partial f_4}{\partial V_T})^{(k)} & (\frac{\partial f_4}{\partial V_M})^{(k)} \\
(\frac{\partial f_5}{\partial I_A})^{(k)} & (\frac{\partial f_5}{\partial I_B})^{(k)} & (\frac{\partial f_5}{\partial I_C})^{(k)} & (\frac{\partial f_5}{\partial I_T})^{(k)} & (\frac{\partial f_5}{\partial I_M})^{(k)} & (\frac{\partial f_5}{\partial V_T})^{(k)} & (\frac{\partial f_5}{\partial V_M})^{(k)} \\
(\frac{\partial f_6}{\partial I_A})^{(k)} & (\frac{\partial f_6}{\partial I_B})^{(k)} & (\frac{\partial f_6}{\partial I_C})^{(k)} & (\frac{\partial f_6}{\partial I_T})^{(k)} & (\frac{\partial f_6}{\partial I_M})^{(k)} & (\frac{\partial f_6}{\partial V_T})^{(k)} & (\frac{\partial f_6}{\partial V_M})^{(k)} \\
(\frac{\partial f_7}{\partial I_A})^{(k)} & (\frac{\partial f_7}{\partial I_B})^{(k)} & (\frac{\partial f_7}{\partial I_C})^{(k)} & (\frac{\partial f_7}{\partial I_T})^{(k)} & (\frac{\partial f_7}{\partial I_M})^{(k)} & (\frac{\partial f_7}{\partial V_T})^{(k)} & (\frac{\partial f_7}{\partial V_M})^{(k)}
\end{bmatrix} \tag{20}$$

(a) Two-phase balanced fault: short circuit faults in both phase T and phase M.

There are short circuit faults at the 27.5 kV phase M and phase T. Then $y_T = y_M = 0.01$

(b) Single-phase unbalanced fault: short circuit fault in phase T or phase M.

There is a short circuit fault at either the 27.5 kV phase T or phase M.

(1) Short circuit fault occurs at phase-T. Then $y_T = 0.01$

(2) Short circuit fault occurs at phase-M. Then $y_M = 0.01$

The following equation considers the single-phase unbalanced fault at the phase T of the power system with the V-V scheme as an example. The function can be obtained by Eq.(13).

$$f(X) = C \tag{21}$$

The above function is rearranged and written as Eq.(17)

If $X^{(k)}$ is an initial estimate of the variable X, the following iterative sequence is formed Eq. (18).

At the initial stage, let the estimate of the current to be

$$\begin{bmatrix} I_A{}^{(0)} \\ I_B{}^{(0)} \\ I_C{}^{(0)} \\ I_T{}^{(0)} \\ I_M{}^{(0)} \\ V_T{}^{(0)} \\ V_M{}^{(0)} \end{bmatrix} = \begin{bmatrix} 0 \\ 0 \\ 0 \\ 0 \\ 0 \\ 0 \\ 0 \end{bmatrix} \tag{22}$$

A solution was obtained when the difference between the absolute value of the successive iteration is less than a specified error tolerance.

$$\left| X^{(k+1)} - X^{(k)} \right| \le \varepsilon \tag{23}$$

where ε is the desired error tolerance.

At stage k, when the current matrix $\begin{bmatrix} I_A{}^{(k)} \\ I_B{}^{(k)} \\ I_C{}^{(k)} \\ I_T{}^{(k)} \\ I_M{}^{(k)} \end{bmatrix}$ is known, the bus voltage matrix $\begin{bmatrix} V_A{}^{(k)} \\ V_B{}^{(k)} \\ V_C{}^{(k)} \\ V_T{}^{(k)} \\ V_M{}^{(k)} \end{bmatrix}$ can be obtained by Eq. (15).

Then the current matrix can by updated by Eq. (18). The other equations Eq. (17), Eq. (19) and Eq. (20) was used. The iteration is repeated until the error between stage k+1 and stage k is acceptable.

2.2.1 Effect of Over-Current Relay

If the voltage sag is caused by a fault in the power system, the duration (△t) depends on the fault clearing time during which the protective relay and the circuit breaker (CB) operate. The relay in consideration is the over-current relay (50/51). The operating time of the relay is obtained from the movement curve. The operating time of the circuit breaker is related to the mechanical characteristic and can be regarded as having a constant value. The duration of voltage sag can be expressed as

$$\Delta t = t_{Ry} + t_{CB} \tag{24}$$

where t_{Ry}: protective relay operating time.

t_{CB}: circuit breaker operating time.

In a practical distribution system, t_{CB} is between 3 and 8 cycles.

According to the IEC 60255-22 Standard, the over current relay (51) inverse t-I curve parameters are given in Eq. (25). The α and β values in Table 1 determine the slopes.

$$t_{Ry}(s)=\frac{k\beta}{\left(\frac{I_F}{I_P}\right)^{\alpha}-1} \tag{25}$$

where k : time multiplier

I_F: fault current detected by relay (normally the effective value).

I_P : current setting threshold.

If the normal inverse curve is used, then α=0.02, and β=0.14 can be substituted into Eq. (25) to yield the voltage sag duration. The value of $\triangle V_{(F)}\triangle t_{(F)}$ can be used to describe the voltage sag range where $\triangle V_{(F)}$ is the drop of voltage, and $\triangle t_{(F)}$ is the duration. From Fig. 10, it can be obtained that

$$\Delta V_{(F)}=V_{SFi}-\frac{I_{Fi}}{y_{src}} \tag{26}$$

where $i=A,B,and\ C$. If $I_{Fi}\geq I_p$, then

$$\Delta t_{(F)}=\frac{0.14k}{\left|\frac{I_{Fi}}{I_P}\right|^{0.02}-1} \tag{27}$$

2.2.2 Voltage Sag Analysis Procedure

Fig. 11 shows the flowchart for the calculation of voltage sag. It is described as follows.

1. System equipment impedances are transformed to pu values, and input equipment parameters data.
2. Select equation for fault voltages and currents at all voltage levels are calculated, and the ranges of voltage sag $\triangle V_{(F)}$ are obtained.
3. Choose the curve of the over-current relay (50/51). The relay operating time and the circuit breaker operating time are added to yield the fault clearing time, which is the voltage sag duration $\triangle t_{(F)}$.
4. Compare $\triangle V_{(F)}$ and $\triangle t_{(F)}$ with the ITI (CBEMA) curve.
5. The voltage sags satisfy requirement with ITI (CBEMA) curve.
6. If is not satisfy, then using ADHDE to compute transformer impedance and relay settings.
7. That is repeated until the voltage sag and duration are acceptable by change transformer impedance and reset relay parameter.

2. 3 Problem Formulation

The ADHDE approach is used to obtain the optimal transformer impedances and relay settings. It is described as follows.

2.3.1 Objective function

$$\text{Minimize}\quad M=\sum\left|V_{unacceptable-point}-V_{ITI-curve}\right| \tag{28}$$

Variable vector: $X=\left[X_{TRS}\quad X_{TRL}\quad k\right]^t$

$$k^{min}<k<k^{max}$$

$$X_{TRi}^{min}<X_{TRi}<X_{TRi}^{max}\qquad i=S,L \tag{29}$$

where k : relay time multiplier

X_{TRS} and X_{TRL} : transformer impedance

2.3.2 Constraints

1. System equipment parameter: The limit conditions of system equipment should be examined.
2. Voltage regulation: The voltage regulation must be less than 5%.

$$-5\%<VR_i<5\%\qquad i=A,B,C \tag{30}$$

3. Coordination of protective relay: The action time of a downstream relay must be less than that of the upstream relay.

$$T_{F,27.5kV}<T_{F,69kV} \tag{31}$$

3. Results

Two-phase balanced faults and single-phase unbalanced faults are considered. Fig. 9 shows the simulation system, whose parameters are given in Table 2 The relay follows the normal inverse curve, where α is 0.02 and β is 0.14. Table 3 gives the original settings.

Table 4 shows the calculation results of the 69kV bus voltages when a two-phase balanced fault occurs at the 27.5kV

bus for the system with the original settings. Fig. 12 gives the comparison of the voltage sag values with the ITI curve. It can be found that with the original settings, the voltage sag values at the 69 kV bus are below the curve.

The ADHDE approach is used to determine the suitable values of transformer impedances and relay k values. Table 5 gives the original settings and limitation conditions. Table 6 gives the optimal parameter values X_{TRS}=7%, X_{TRL}=16%, and k=0.01 was determined by using the ADHDE approach. Table 7 shows the calculation results of the 69kV bus for the system with parameter values determined by the ADHDE approach. At the V_A (V-V) phase, table 7 shows that the fault voltage, fault current, fault clearing time, and objective function are 0.6456 p.u., 14.41 p.u., 0.10554 s, and 0.0543 p.u., respectively. Although the V_A (Le Blanc) phase objective function is as high as 0.0833 p.u., fault voltage, fault current, fault clearing time are satisfied. Because both the emigrant and accelerated operations are embedded in ADHDE, a global optimum and faster convergence are achieved.

They are compared with the ITI curve as plotted in Fig. 12. When the transformer impedances and relay settings are modified by using the ADHDE approach, the voltage values have been raised using system faults. A short circuit fault occurs in phase T at the 27.5kV bus, as displayed in Fig. 10, will be examined.

Table 8 shows the results of the 69kV bus for the system with the original setting. At the V_B (V-V) phase, table 8 shows that the fault voltage, fault current, fault clearing time, and objective function are 0.5322 p.u., 17.09 p.u., 0.2397 s, and 0.3197 p.u., respectively. Although the V_B (Le Blanc) phase objective function is as high as 0.3703 p.u., the fault voltage, fault current, fault clearing time are satisfied. The voltage sag values at the 69kV bus are also compared with the ITI curve, as plotted in Fig. 12. Table 9 presents the simulation results of the 69kV bus for the system with parameter values determined by the ADHDE approach. The 69kV bus voltage values are also compared with the ITI curve as plotted in Fig. 13. It is found that the both V_B ,V_C (Scott), and V_B ,V_C (Le Blanc) voltage sag values of 69kV bus are not satisfied with the ITI curve of the system suffering a single-phase unbalanced fault. Hence, the voltage sag severity also has been improved.

4. Conclusions

A study of modeling of specially connected transformers using the optimal planning of voltage sag in a power system considering ITI curve was introduced. Then the voltage sag severity of a system with specially connected transformers can be controlled by adjusting the transformer impedances and relay settings. In this paper, balanced two-phase short-circuit faults and unbalanced single-phase short-circuit faults are used to investigate the problems of voltage sag. The three connection schemes which V-V, Scott and Le Blanc connection, and node admittance matrix of each scheme is obtained for voltage sag calculation. This paper presents an ADHDE optimization approach for solving the suitable transformer impedances and relay settings values. The results are also compared with the ITI curve. Finally, simulation results show that the voltage sag can be improved by the proposed method.

In addition, the proposal models can be easily implemented into the voltage unbalance system to improved voltage sag program studies, and then the effects of large unbalanced specially connected transform system demands on the power supply can be simulated accurately. The studies can be increase acceptable effects of voltage sag for the large unbalance loading condition.

References

Bollen, M. H. J. (1999). Understanding power quality problems：Voltage sags and interruptions. *IEEE Press Series on Power Engineering, IEEE*, New York, USA.

Bollen, M. H. J. (1995). The influence of motor reacceleration on voltage sags. *IEEE Transactions on Industry Applications*, *31*(4), 667 -674.

Bollen, M. H. J. (1997). Characterization of voltage sags experienced by three-phase adjustable-speed drives. *IEEE Transactions on Power Delivery*, *12*(4), 1666 -1671.

Chang, Y. P., & Wu, C. J. (2005). Optimal multi-objective planning of large-scale passive harmonic filters using hybrid differential evolution method considering parameter and loading uncertainty. *IEEE Transactions on Power Delivery*, *20*(1), 408-416.

Chen, T. H. (1994). Simplified models of electric substations for three-phase power-flow studies. Paper presented in the IEEE Proceeding of the 29th IAS Annual Meeting, Denver, Colorado, USA.

Chen, T. H., & Kuo, H. Y. (1995). Network modeling of traction substation transformers for studying unbalance effects. *IEE Proceedings- Generation Transmission and Distribution*, *142*(2), 103-108.

Chiou, J. P., & Wang, F. S. (1998). A hybrid method of differential evolution with application to optimal control problems of a bioprocess system. Paper presented in the IEEE Proceeding of the IEEE Evolutionary Computation Conference, Anchorage, Alaska, U.S.A.

Chang, Y. P., & Low, C. Y. (2008). An ant direction hybrid differential evolution heuristic for the large-scale passive harmonic filters planning problem. *Expert Systems with Applications*, *35*(3), 894-904.

Conrad, L. E., & Bollen, M. H. J., (1997). Voltage sag coordination for reliable plant operation. *IEEE Transactions on Industry Applications*, *33*(6), 1459 -1464,

Das, J. C. (1990). Effects of momentary voltage dips on the operation of induction and synchronous motors. *IEEE Transactions on Industry Applications*, *26*(4), 711 -718.

Gomez, J. C., & Morcos, M. M. (2002). Coordinating overcurrent protection and voltage sag in distributed generation system. *IEEE Power Engineering Review*, *22*(2), 16-19.

Gomez, J. C., & Morcos, M. M. (2002). Voltage sag and recovery time in repetitive events. *IEEE Transactions on Power Delivery*, *17*(4), 1037-1043.

Heydt, G. T., & Jewell, W. T. (1998). Pitfalls of electric power quality indices. *IEEE Transactions on Power Delivery*, *13*(2), 570-578.

Heydt, G. T., Ayyanar, R., & Thallam, R. (2001). Power acceptability. *IEEE Power Engineering Review*, *21*(9), 12-15.

Huang, S. R., Kuo, Y. L., Chan, B. N, Lu, K. C., & Huang, M. C. (2001) .A short circuit current study for the power supply system of Taiwan railway. *IEEE Transactions on Power Delivery*, *16*(4), 492-497.

IEC Standard 60255-22 (2007). *IEC recommended practice for single input energizing quality measuring relay with dependent or independent time*. New York: The Institute of Electrical and Electronics Engineers.

IEEE Standard 446 (1990). *IEEE recommended practice for emergency and standby power systems for industrial and commercial applications.* New York: The Institute of Electrical and Electronics Engineers.

IEEE Standard 1100 (2005). *IEEE recommended practice for powering and grounding electronic equipment*. New York: The Institute of Electrical and Electronics Engineers.

IEEE Standard 1159 (1995). *IEEE recommended practice for monitoring electric power quality*. New York: The Institute of Electrical and Electronics Engineers.

Kyei, J., Ayanar, R., Heydt, G., & Thallam, R. (2002). The design of power acceptability curves. *IEEE Transactions on Power Delivery*, *17*(3), 828-833.

Lee, G. J., Albu, M. M., & Heydt, G. T. (2004). A power quality index based on equipment sensitivity, cost, and network vulnerability. *IEEE Transactions on Power Delivery*, *19*(3), 1504-1510.

Lin ,Y. C., Hwang, K. S., & Wang, F. S. (2000). *Plant scheduling and planning using mixed-integer hybrid differential evolution with multiplier updating*. Paper presented in the IEEE Proceeding on Evolutionary Computation Conference, Chicago, Illinois, USA.

Lin, Y. C., Wang, F. S., & Hwang, K. S. (1999). *A hybrid method of evolutionary algorithms for mixed-integer optimization problems*. Paper presented in the IEEE Proceeding on Evolutionary Computation Conference, Washington D.C., USA.

Yalcinkaya, G., Bollen, M. H. J., & Crossley, P. A. (1998). Characterization of voltage sags in industrial distribution systems. *IEEE Transactions on Industry Applications*, *34*(4), 682 -688.

Table 1 Inverse t-I curve parameter of over-current relay

	t-I curve setting	α	β
A	Normal Inverse	0.02	0.14
B	Very Inverse	1.0	13.5
C	Extremely Inverse	2.0	80.0
D	Long-Time Inverse	1.0	120.0

Table 2 System data

Power Source	Balanced three-phase, 161 kV, Y-connected, X/R=33.25, short circuit capacity=10935 MVA
Transformer	TRS：3Φ/3Φ, 161/69 kV, 200 MVA, X_{TRS}=13%, X/R=40, △/Y-g connected, Z_{g1}=20 Ω TRL：3Φ/2Φ, 69/27.5 kV, 30 MVA, X_{TRL}=10%, X/R=10
Line	Z_{L1}=1.1869+j3.9108 Ω Z_{L2T}= Z_{L2M}=0.97+j2.55 Ω
Load	Each of phase T and phase M: 5MW+j3MVAR
Circuit breaker	T_{CB}=0.08 s

Table 3 Original setting of protection relay inverse t-I curve

Voltage level	Time multiple (k)
27.5 kV	0.1
69 kV	0.2

Table 4 Calculation results of 69kV bus for two-phase balanced fault at 27.5kV bus of system with original parameter settings （t_{CB}=0.08s）

Phase	Fault voltage (p.u.)	Fault current (p.u.)	Relay operating time t_{Ry} (s)	Fault clearing time △t (s)
V_A(V-V)	0.5294	17.60	0.2371	0.3171
V_B(V-V)	0.3010	22.66	0.2174	0.2974
V_C(V-V)	0.5000	15.89	0.2462	0.3262
V_A(Scott)	0.3886	19.97	0.2269	0.3069
V_B(Scott)	0.3321	22.44	0.2181	0.2981
V_C(Scott)	0.3113	22.03	0.2194	0.2994
V_A(Le Blanc)	0.3426	21.45	0.2214	0.3014
V_B(Le Blanc)	0.3406	21.53	0.2211	0.3011
V_C(Le Blanc)	0.3401	21.51	0.2211	0.3011

Table 5 Original settings and limitation conditions

	System parameter	Original setting	Limitation
Power sourec	TRS 3Φ/3Φ 161/69 kV 200 MVA	X_{TRS}=13%	7%<X_{TRS}<13%
Transformer	TRL 3Φ/2Φ 69/27.5 kV 30 MVA	X_{TRL}=10%	10%<X_{TRL}<16%
Relay	CO-k	k=0.1	0.01<k<0.1

Table 6 Determined parameter values using ADHDE

X_{TRS}	X_{TRL}	k
7%	16%	0.01

Table 7 Calculation results of 69kV bus for two-phase balanced fault at 27.5kV bus of system with parameter values determined by ADHDE（t_{CB}=0.08s）

Phase	Fault voltage (p.u.)	Fault current (p.u.)	Fault clearing time △t (s)	Objective function (p.u.)
V_A(V-V)	0.6456	14.41	0.10554	0.0543
V_B(V-V)	0.4147	19.95	0.10269	0.0827
V_C(V-V)	0.6087	13.11	0.10651	0.0865
V_A(Scott)	0.5108	16.79	0.10412	0.0841
V_B(Scott)	0.4453	19.72	0.10279	0.0828
V_C(Scott)	0.4227	19.33	0.10294	0.0829
V_A(Le Blanc)	0.4599	18.51	0.10329	0.0833
V_B(Le Blanc)	0.4576	18.60	0.10325	0.0832
V_C(Le Blanc)	0.4571	18.59	0.10326	0.0833

Table 8 Calculation results of 69kV bus for a single-phase unbalanced fault (phase T) at 27.5kV Bus of system with original parameter settings (t_{CB}=0.08s)

Phase	Fault voltage (p.u.)	Fault current (p.u.)	Relay operating time t_{Ry} (s)	Fault clearing time △t (s)
V_A(V-V)	0.6657	17.18	0.2392	0.3192
V_B(V-V)	0.5322	17.09	0.2397	0.3197
V_C(V-V)	0.9923	0.28	-	-
V_A(Scott)	0.3886	19.97	0.2269	0.3069
V_B(Scott)	0.8357	9.80	0.2998	0.3798
V_C(Scott)	0.9233	10.17	0.2949	0.3749
V_A(Le Blanc)	0.3426	21.45	0.2214	0.3014
V_B(Le Blanc)	0.8309	10.54	0.2903	0.3703
V_C(Le Blanc)	0.9185	10.92	0.2859	0.3659

Table 9 Calculation results of 69kV bus for a single-phase unbalanced fault (Phase T) at 27.5kV bus of system with parameter values determined by ADHDE (t_{CB}=0.08s)

specially connected transformers	Fault voltage (p.u.)	Fault current (p.u.)	Fault clearing time △t (s)	Objective function (p.u.)
V_A(V-V)	0.7239	14.39	0.10556	0.0239
V_B(V-V)	0.6087	14.31	0.10561	0.0856
V_C(V-V)	0.9923	0.28	-	-
V_A(Scott)	0.5108	16.79	0.10412	0.0841
V_B(Scott)	0.8545	8.22	0.11253	0.0925
V_C(Scott)	0.9363	8.58	0.11188	0.0919
V_A(Le Blanc)	0.4599	18.51	0.10329	0.0833
V_B(Le Blanc)	0.8457	9.08	0.11103	0.0910
V_C(Le Blanc)	0.9308	9.44	0.11048	0.0905

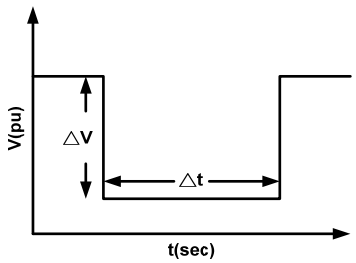

Fig. 1. Voltage sag characteristics.

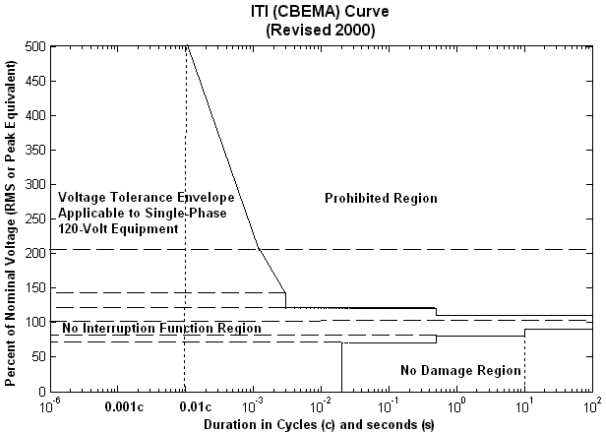

Fig. 2. ITI (CBEMA) curve.

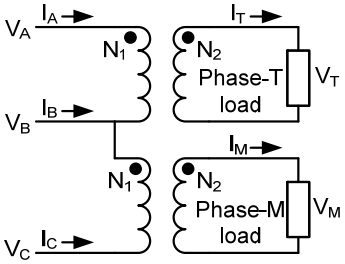

Fig. 3. V-V connection scheme.

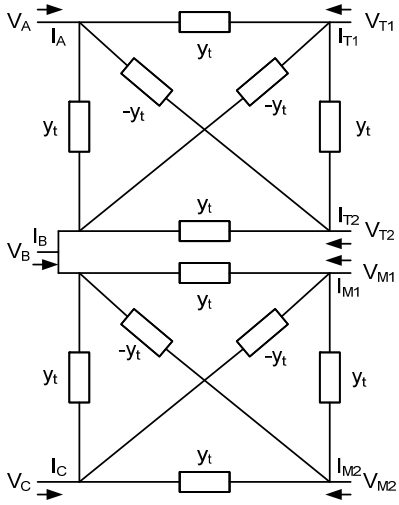

Fig. 4. Equivalent circuit of V-V connection scheme.

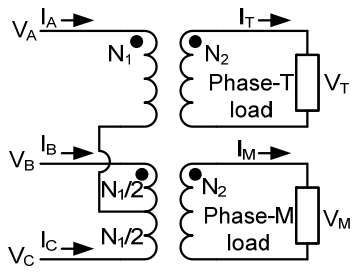

Fig. 5. Scott connection scheme.

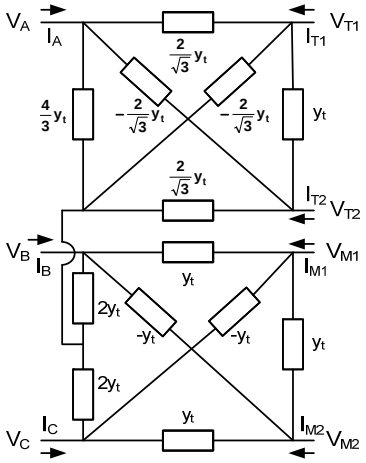

Fig. 6. Equivalent circuit of Scott connection scheme.

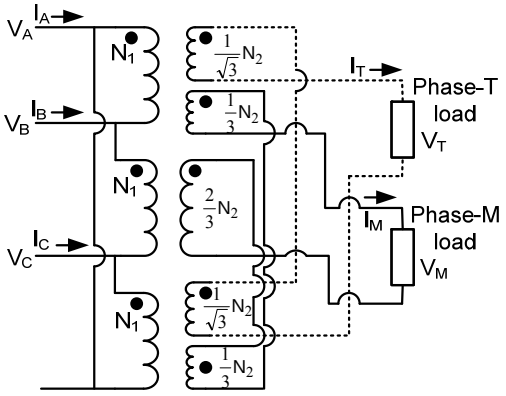

Fig. 7. Le Blanc connection scheme.

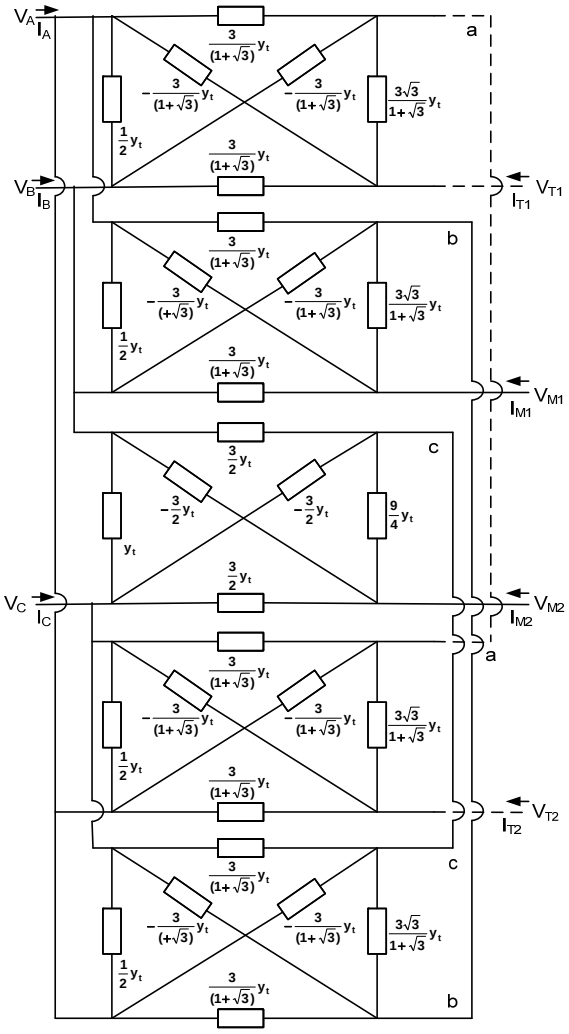

Fig. 8. Equivalent circuit of Le Blanc connection scheme.

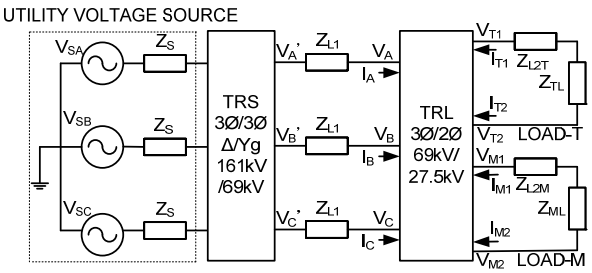

Fig. 9. A power system with specially connected transformers.

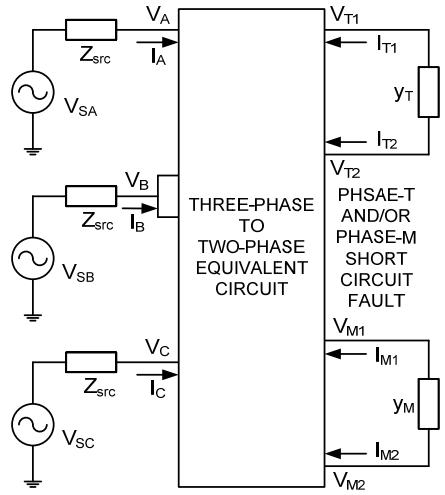

Fig. 10. Short circuit analysis of a power system with specially connected transformers.

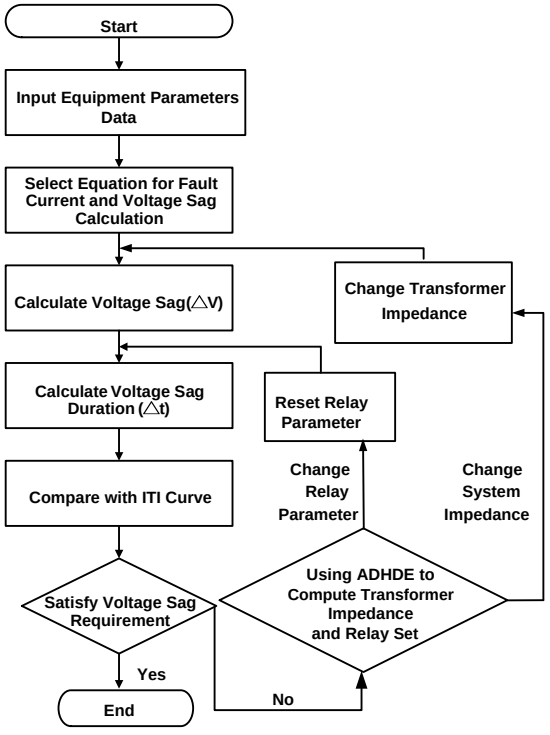

Fig. 11. Voltage sag calculation flowchart.

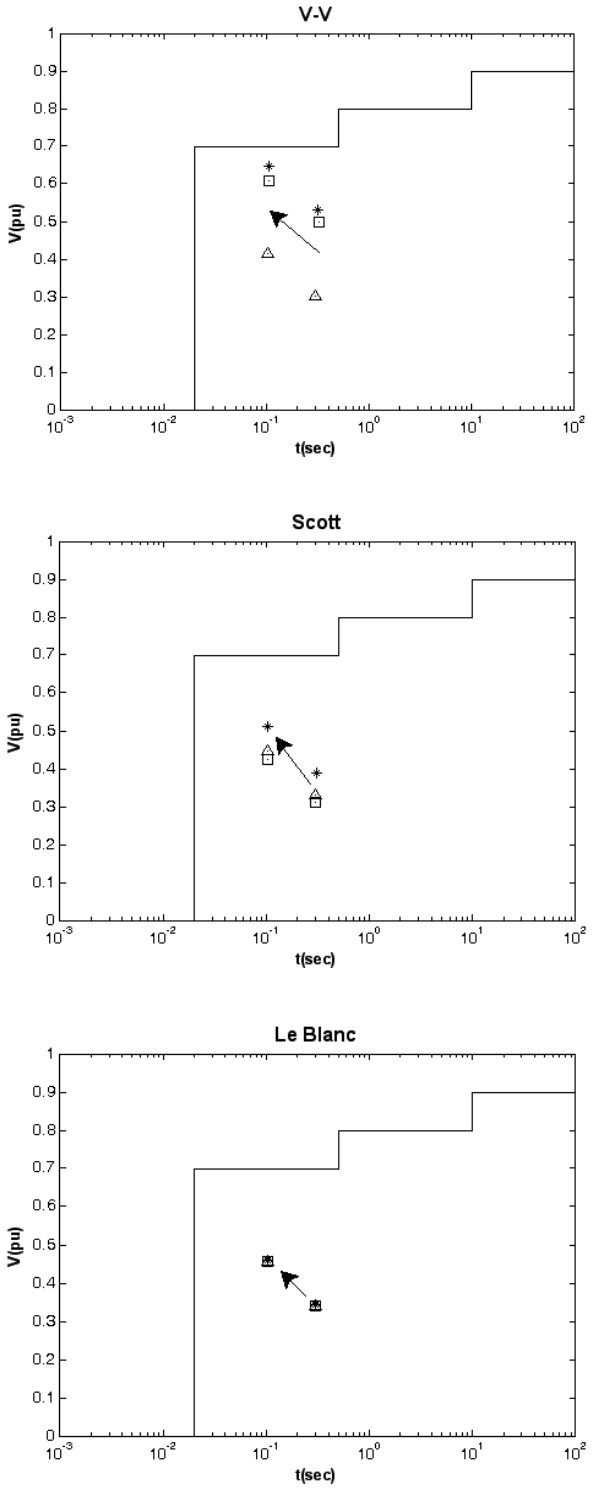

Fig. 12. Comparison of voltage sag values of 69kV bus with ITI curve of the system suffering a two-phase balanced fault at 27.5kV bus and with parameter settings determined by original and ADHDE (star : V_A, triangle : V_B, square : V_C).

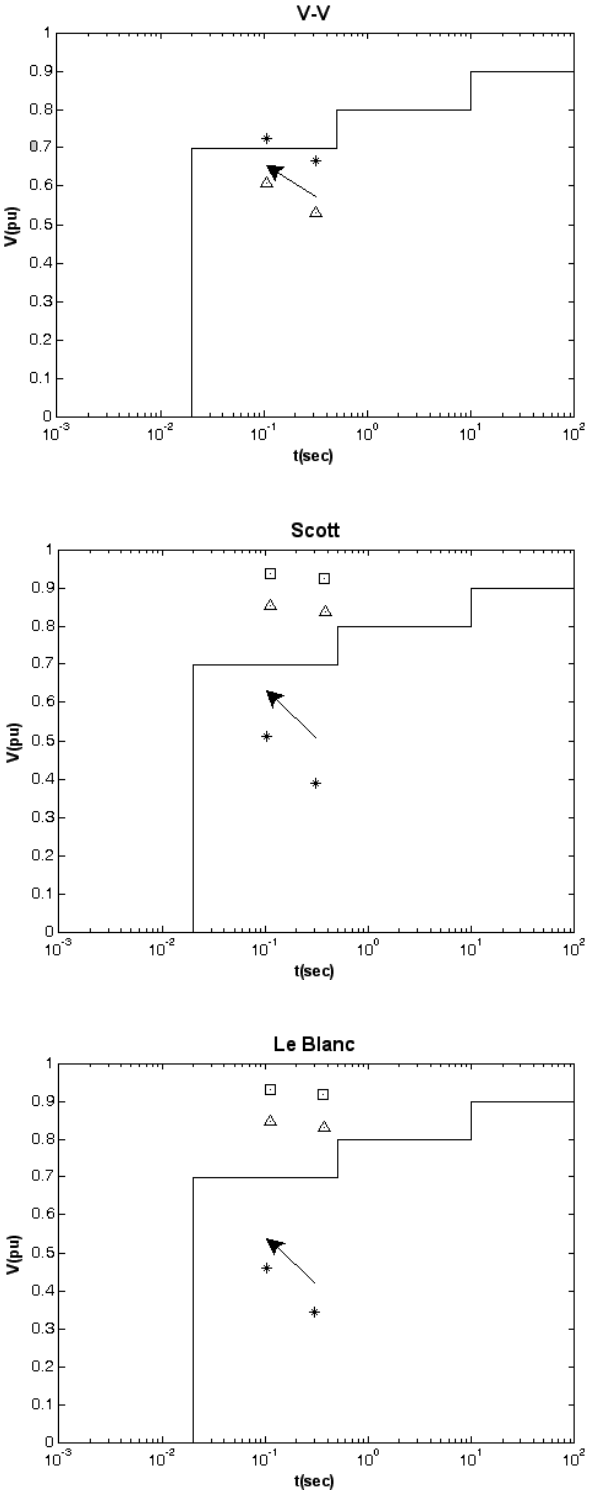

Fig. 13. Comparison of voltage sag values of 69kV bus with the ITI curve of the system suffering a single-phase unbalanced fault (phase T) at 27.5kV bus and with parameter values determined by original and ADHDE (star : V_A, triangle : V_B, square : V_C).

Appendix

Method for ant direction hybrid differential evolution (ADHDE) can be expressed as follows:

A nonlinear constrained optimization problem can be expressed as

Minimize $M(\underline{X})$ (A1)

Subject to

$$g_k(\underline{X}) \le 0 \qquad k = 1,..., n_g \tag{A2}$$

$$h_k(\underline{X}) = 0 \qquad k = 1,..., n_h \tag{A3}$$

where $M(\underline{X})$: objective function of variable vector $\underline{X}$,

$$\underline{X} = \left[X_1, X_2, .., X_j, .., X_D\right]^t$$

$g_k(\underline{X})$: inequality constraints.

$h_k(\underline{X})$: equality constraints.

The ADHDEOA is a method combining both an ant direction hybrid differential evolution and orthogonal arrays for minimizing nonlinear and non-differential objective functions. The ACS used in the ADHDE is mainly for finding the proper mutation operations to speed up convergence toward a global solution. Unlike the approach from Dorigo and Gambardella, the difference between the objective value in the next generation and the best objective value of the present generation constructs a fluctuant pheromone quality. Orthogonal array is a systematic and time-efficient approach that can aid in experimental design. Here an orthogonal array is applied to search for the best initial point in the search space. The ADHDE is then applied to search for the optimum design of a passive filter. In practice, the construction of objective function comprises four parts: total harmonic distortion of the voltage, total demand distortion of harmonic, total filter loss and the cost of filters. In addition, a membership function is provided for dealing with the weight of each objective in this study.

The entire search flowchart is shown in Fig.1. The solution procedures are stated in detail as follows.

Step 1. Initialization

To increase convergence speed and achieve a global optimum, the orthogonal array is initially applied to determine the starting point. Next, the ADHDE finds the (Np-1) random initial vectors. The main key-operations of the ADHDE are shown as follows:

The initial populations $\underline{X}_i^0$, $i = 1,2,...,(N_p - 1)$, chosen randomly, should cover the entire search space uniformly. The elements of individual $\underline{X}_i^0$ are given by

$$X_{ji}^0 = X_j^{min} + \rho_i (X_j^{max} - X_j^{min}) , \; j = 1,2,..., D \;, i = 1,2,...,(N_p - 1) \tag{A4}$$

where $\rho_i \in [0,1]$ is a random number; X_j^{min} and X_j^{max} are the lower and upper bounds of the variable, respectively.

Step 2. Mutation operation

In the mutation process, five mutation operations are evaluated and the proper one determined through an ACS (see Section 2.2) search process. The operations are introduced, as follows:

(1) Scheme MO1

For each vector $\underline{X}_i^G, i = 1,2,...,N_p$, a mutant vector $\underline{U}_i^{G+1}$ is generated according to

$$\underline{U}_i^{G+1} = \underline{X}_{r1}^G + F(\underline{X}_{r2}^G - \underline{X}_{r3}^G), \; i = 1,2,...,N_p \tag{A5}$$

where r_1, r_2 and r_3 are chosen randomly from the interval $(1, N_P)$ and differ from the running index i; $F \in [0,1]$ is a scalar factor.

(2) Scheme MO2

At generation G, a mutant vector is generated on the basis of the present individual $\underline{X}_i^G$ by

$$\underline{U}_i^{G+1} = \underline{X}_i^G + F(\underline{X}_{r1}^G - \underline{X}_{r2}^G), \; i = 1,2,...,N_p \tag{A6}$$

where $i \ne r1, \; i \ne r2$ and $r1, r2 \in \{1,2,...N_p\}$; $F \in [0,1]$ is a scalar factor; $\underline{X}_{r1}^G$ and $\underline{X}_{r2}^G$ are two randomly selected individuals.

(3) Scheme MO3

Basically, Scheme MO3 works the same way as Scheme MO2 but generates $\underline{U}_i^{G+1}$ according to

$$\underline{U}_i^{G+1} = \underline{X}_i^G + F[(\underline{X}_{r1}^G - \underline{X}_{r2}^G) + (\underline{X}_{r3}^G - \underline{X}_{r4}^G)], \; i = 1,2,...,N_p \tag{A7}$$

The mutation process at the Gth generation begins by randomly selecting four population individuals $\underline{X}_{r1}^G$, $\underline{X}_{r2}^G$, $\underline{X}_{r3}^G$ and $\underline{X}_{r4}^G$.

(4) Scheme MO4

Scheme MO4 comprises two pair difference vectors based on the present individual $\underline{X}_i^G$ by

$$\underline{U}_i^{G+1} = \underline{X}_i^G + [\lambda(\underline{X}_b^G - \underline{X}_i^G) + F(\underline{X}_{r1}^G - \underline{X}_{r2}^G)],\ i = 1,2,...,N_p \quad \text{(A8)}$$

in which $\underline{X}_{r1}^G$ and $\underline{X}_{r2}^G$ are two randomly selected individuals, and $\underline{X}_b^G$ is the best individual. In general, variable λ is set to F for computation sake.

(5) Scheme MO5

Scheme MO5 works the same way as Scheme MO3, but a mutant vector is generated on the basis of the random present individual $\underline{X}_{r1}^G$ by

$$\underline{U}_i^{G+1} = \underline{X}_{r1}^G + F[(\underline{X}_{r2}^G - \underline{X}_{r3}^G) + (\underline{X}_{r4}^G - \underline{X}_{r5}^G)],\ i = 1,2,...,N_p \quad \text{(A9)}$$

in which $\underline{X}_{r1}^G$, $\underline{X}_{r2}^G$, $\underline{X}_{r3}^G$, $\underline{X}_{r4}^G$ .and $\underline{X}_{r5}^G$ are five randomly selected individuals.

Step 3. Crossover operation

To extend the diversity of individuals in the next generation, the perturbed individual $\underline{U}_i^{G+1} = \left[U_{1i}^{G+1}, U_{2i}^{G+1}, .., U_{ji}^{G+1}, .., U_{Di}^{G+1}\right]^t$ and the present individual $\underline{X}_i^G = \left[X_{1i}^G, X_{2i}^G, .., X_{ji}^G, .., X_{Di}^G\right]^t$ are mixed to yield the trial vector

$$\underline{\hat{U}}_i^{G+1} = \left[\hat{U}_{1i}^{G+1}, \hat{U}_{2i}^{G+1}, .., \hat{U}_{ji}^{G+1}, .., \hat{U}_{Di}^{G+1}\right]^t \quad \text{(A10)}$$

where

$$\hat{U}_{ji}^{G+1} = \begin{cases} X_{ji}^G, if \quad a\ random\ \ number > C_R \\ U_{ji}^{G+1}, otherwise \end{cases}$$

$$j = 1,2,....., D\ , i = 1,2,..., N_P \quad \text{(A11)}$$

where D is also the number of genes. Since $C_R \in [0,1]$ is the crossover factor, it must be set by the user.

Step 4. Evaluation and selection

The parent is replaced by its offspring in the next generation if the fitness of the latter is better; otherwise, the parent is retained. The first step is a one-to-one competition. The next step selects the best individual, $\underline{X}_b^{G+1}$ in the population. That is,

$$\underline{X}_i^{G+1} = \text{arg-min}\{M(\underline{X}_i^G), M(\underline{\hat{U}}_i^{G+1})\}, i = 1,2,..., N_P \quad \text{(A12)}$$

$$\underline{X}_b^{G+1} = \text{arg-min}\{M(\underline{X}_i^{G+1})\}, i = 1,2,..., N_P \quad \text{(A13)}$$

where arg-min denotes the argument of the minimums.

The foregoing steps are repeated until the maximum iteration number or the desired fitness is achieved. In general, a faster descent usually leads to a local minimum or a premature convergence. Conversely, diversity guarantees a high probability of obtaining the global optimum. A trade-off can be achieved by slightly lowering the scaling factor *F* and by increasing the population size *Np* ; however, more computation time is required. The migrant and accelerated operations in HDE are used to overcome the local minimum solution and time consumption. The migrant and accelerating operations are embedded in the original DE.

Step 5. Migrant operation (if necessary)

To increase search space exploration, a migration operation is introduced to regenerate a diverse population of individuals. The migrant individuals are chosen on a “best individual” basis $\underline{X}_b^{G+1}$. The j[th] gene of $\underline{X}_i$ is regenerated by

$$X_{ji}^{G+1} = \begin{cases} X_{jb}^{G+1} + \rho_1(X_j^{\min} - X_{jb}^{G+1}),\ if\ \ \rho_2 < \dfrac{X_{jb}^{G+1} - X_j^{\min}}{X_j^{\max} - X_j^{\min}} \\ X_{jb}^{G+1} + \rho_1(X_j^{\max} - X_{jb}^{G+1}),\ otherwise \end{cases} \quad \text{(A14)}$$

where ρ_1 and ρ_2 are randomly generated numbers uniformly distributed in (0,1). The migrant population will not only become a set of newly promising solutions but also avoid the local minimum trap.

The migrant operation is performed only if a measure fails to match the desired population diversity tolerance. The measure in this study is defined as

$$u = \frac{\left[\sum_{\substack{i=1 \\ i \neq b}}^{N_P} \sum_{j=1}^{D} \eta_{ji}\right]}{D(N_P - 1)} < \varepsilon_1 \quad \text{(A15)}$$

where

$$\eta_{ji} = \begin{cases} 1,\ if\ \ \left|\dfrac{X_{ji}^{G+1} - X_{jb}^{G+1}}{X_{jb}^{G+1}}\right| > \varepsilon_2 \\ 0,\ otherwise \end{cases} \quad \text{(A16)}$$

Parameters $\varepsilon_1 \in (0,1)$ and $\varepsilon_2 \in (0,1)$ express the desired tolerance of the population diversity and the gene diversity with

regard to the best individual, respectively. Here η_{ji} is defined as an index of the gene diversity. A zero η_{ji} indicates means that the j^{th} gene of the i^{th} individual is close to the j^{th} gene of the best individual. If the degree of population diversity u is smaller than ε_1, the HDE performs a migration to generate a new population to escape the local point. Otherwise, the HDE breaks off the migration, thereby maintaining an ordinary search direction.

Step 6. Accelerated operation (if necessary)

When the fitness in the present generation is no longer improved by using the mutation and crossover operations, a descent method is then applied to push the present best individual toward a better point. Thus, the acceleration operation can be expressed as

$$\underline{\hat{X}}_b^{G+1} = \begin{cases} \underline{X}_b^{G+1}, & if \quad M(\underline{X}_b^{G+1}) < M(\underline{X}_b^{G}) \\ \underline{X}_b^{G+1} - \alpha \nabla M(\underline{X}_b^{G+1}), & otherwise \end{cases} \tag{A17}$$

The gradient of the objective function, $\nabla M(\underline{X}_b^{G+1})$, can be calculated approximately with a finite difference. The step size $\alpha \in (0,1]$ is determined according to the decent property. First, α is set at unity. The objective function $M(\underline{\hat{X}}_b^{G+1})$ is then compared with $M(\underline{X}_b^{G+1})$. If the decent property is achieved, $\underline{\hat{X}}_b^{G+1}$ becomes a candidate in the next generation and is added into this population to replace the worst individual. On the other hand, if the decent requirement fails, the step size is reduced to, for example, 0.5 or 0.7. The decent search method is repeated to find the optimal $\underline{\hat{X}}_b^{G+1}$, called $\underline{X}_b^N$, at the $(G+1)^{th}$ generation. This result shows that the objective function $M(\underline{X}_b^N)$ should be at least equal to or smaller than $M(\underline{X}_b^{G+1})$.

考量資訊技術產業曲線含特殊變壓器連接之電力系統電壓驟降最佳規劃

張英彬

南開科技大學　電機工程系

摘　要

本論文針對具有 V-V、史考特與 Le Blanc 特殊變壓器連接的電力系統，利用蟻行混合差分進化法(ADHDE) 進行電壓驟降最佳規劃。文中主要是同時考量資訊技術產業曲線（電腦商業設備製造商協會曲線）與過電流電驛之間協調性問題。首先提出等效節點導納矩陣模型來計算單相或兩相系統故障發生後電壓驟降的嚴重程度。文中進一步提出分析方程式做爲數學方法和發生平衡、不平衡故障時特殊變壓器聯接的最佳規劃模型。然後，討論電壓驟降發生期間對過電流電驛設定之影響；最後，應用 ADHDE 演算法獲得最佳合適變壓器阻抗值，此外爲驗證所提方法之可行性，本文使用具有 V-V、史考特與 Le Blanc 特殊變壓器連接之電力系統爲實際測試案例，由模擬結果顯示所提方法的有效性，同時對於電壓驟降的嚴重程度可藉由調整變壓器阻抗值和電驛設定能有效改善。最後，本文所提方法 ADHDE 求出最佳的變壓器電抗值 X_{TRS}=7%、系統的電抗值 X_{TRL}=16%和過電流電驛設定 k =0.01，在 69kv 匯流排之相電壓 V_A (V-V)所計算出故障電壓、故障電流、故障清除時間和目標函數分別爲 14.41 p.u.、0.6456 p.u.、0.10554 p.u.和 0.0543 p.u.。雖然相電壓 V_A (V-V) 的目標函數高達 0.0833 p.u.，然而故障電壓、故障電流、故障清除時間也能滿足限制條件。由於遷移及加速運算嵌入在 ADHDE 方法中，以致於能快速的收斂並獲得全域最佳解。

關鍵詞：電壓驟降、電力品質、資訊技術產業曲線（電腦商業設備製造協會）、蟻行混合差分進化法、特殊變壓器連接